OBSERVATIONS OF LANGMUIR WAVES DETECTED BY THE CASSINI SPACECRAFT

G. B. Hospodarsky[*], W. S. Kurth[*], D. A. Gurnett[*], P. Zarka[†], P. Canu[‡], M. K. Dougherty[§], G. H. Jones[¶], A. Coates[‖], and A. Rymer[‖]

Abstract

The multiple gravity assist flybys of the Cassini spacecraft during its seven year journey to Saturn provides a unique opportunity to study and compare similar plasma and radio wave emissions at Venus, Earth, Jupiter, and Saturn. Langmuir waves are one such emission, and were detected by Cassini upstream of the bow shocks of each of these planets. A period of Langmuir wave emissions is examined upstream of the bow shock of each of the four planets using the Radio and Plasma Wave Science (RPWS) instrument. The characteristics of the Langmuir waves are compared and the peak electric field amplitude and energy density ratio are determined. The measured peak electric field amplitudes are similar at each of the four planets. The energy density ratio is found to increase with distance from the sun.

1 Introduction

The Cassini mission to Saturn, with its gravity assist flybys of Venus, Earth, and Jupiter, provides a opportunity to study Langmuir waves, also known as electron plasma oscillations, upstream of the bow shock of four planets with the same spacecraft. Langmuir waves upstream of planetary bow shocks are produced by energetic electrons accelerated at the bow shock escaping into the solar wind. As the electrons stream along the interplanetary magnetic field lines, the solar wind convects the guiding centers of the particles downstream due to the $v_{sw} \times B$ electric field. The electrons originating from the tangent point with the highest energy define a region called the electron foreshock. Due

[*] Dept. of Physics and Astronomy, University of Iowa, Iowa City, IA 52242, USA
[†] Observatoire de Paris, LESIA, UMR CNRS 8109, 92195 Meudon, France
[‡] CETP/UVSQ, Velizy, France
[§] Blackett Lab., Imperial College, London, UK
[¶] Jet Propulsion Laboratory, California Institute of Technology, Pasadena, CA, USA; now at Max-Planck-Institut für Sonnensystemforschung, Katlenburg-Lindau, Germany
[‖] Mullard Space Science Laboratory, Holmbury St. Mary, Dorking, UK

to time-of-flight effects, only the electrons above a certain critical velocity can reach the spacecraft, thereby forming a beam [Filbert and Kellogg, 1979]. The existence of a beam provides the region of positive slope, $\partial f/\partial v$, necessary for generating the Langmuir waves. Electrons below this critical velocity are convected downstream before they can reach the spacecraft.

Langmuir waves observed in association with planetary bow shocks exhibit a great deal of structure and variability. The type of structure observed is usually related to the position of the spacecraft in the foreshock. The Langmuir waves near the tangent field line usually occur in a narrow band in frequency ($\Delta f/f$ of a few percent) near the plasma frequency and are usually very intense (E $\sim$ 10mVm^{-1} at Earth) [Cairns et al. 1997; Bale et al., 1997, 2000; Sigsbee et al., 2004a, 2004b]. As a spacecraft moves deeper into the foreshock region, the Langmuir waves become weaker and more irregular. The spectrum of the Langmuir waves also spreads both upward and downward in frequency, and the bandwidth increases ($\Delta f/f \sim 0.5$) [Etcheto and Faucheux, 1984; Fuselier et al., 1985; Lacombe et al., 1985; Lobzin et al., 2005]. The Langmuir wave emissions observed upstream of planetary bow shocks are also very bursty in nature and show considerable fine structure. At Jupiter the electric field waveforms of Langmuir waves show structure on the order of milliseconds (tens of Debye lengths) [Gurnett et al., 1981]. At Venus, Hospodarsky et al. [1994] reported structures as small as 0.15 ms ($\sim$ 10 Debye lengths). Studies at the Earth have found similar fine-structure in the foreshock region [Hospodarsky, 1996; Sigsbee, et al., 2004b, Soucek et al., 2005] and in the auroral zone [Kinter et al., 1995; Bonnell et al., 1997].

2 Instrument Description

The RPWS consists of five receivers, a Langmuir Probe, three electric antennas, and a triaxial search coil magnetometer (see Gurnett et al. [2004] for a detailed description of the instrument). The RPWS electric antenna system consists of three conducting cylinders, each 10 m long and 2.83 cm in diameter. Usually, two of the elements are used as a dipole antenna with a tip-to-tip length of 18.52 m (effective length of 9.26 m) parallel to the spacecraft x-axis, with the third element used as a 10 m (effective length of 5 m) long monopole antenna perpendicular to the dipole. See Gurnett et al. [2004] for a more detailed discussion and a sketch of the antenna orientation. The receivers cover a range from $\sim$ 1 Hz to 16 MHz for electric fields, and $\sim$ 1 Hz to 12 kHz for magnetic fields. Due to the changing frequency of the Langmuir waves detected at each of the four planets, the high frequency receiver (HFR) data is used for the Venus and Earth flyby analysis, and medium frequency receiver (MFR) data is used at Jupiter and Saturn. The A, B, and C filter bands of the HFR cover a frequency range from 3.5 to 319 kHz. Each filter covers 2.2 octaves in frequency (i.e., a factor of 4.5). Digital spectral analysis is performed within each of the three filter bands to provide 8, 16, or 32 logarithmically spaced frequency channels, yielding spectral resolutions of 20, 10, or 5%, respectively. The high frequency receiver has an automatic gain control (AGC) that provides a dynamic range of about 90 dB. At any specific gain setting of the AGC, the digital spectrum analyzer has a dynamic range of about 30 dB. Since the high frequency receiver is under the control of its own processor, virtually all of the receiver parameters can be selected by command, making for an extremely flexible instrument. During the second Venus flyby, the bands A, B, and C of the HFR were operated with 32 digital logarithmically spaced frequency channels and an integration time of 0.125 seconds. For the Earth flyby Langmuir wave measurements discussed below, bands A, B, and C was operated in the 16 logarithmically spaced frequency channels mode, and a 0.5 seconds integration time.

The medium frequency receiver (MFR) provides intensity measurements from a single selected antenna over a frequency range from 24 Hz to 12 kHz. This receiver is usually operated in a mode that toggles every 32 seconds between either the E_x electric dipole or E_w monopole antenna, and the B_x or B_z magnetic search coil. The medium frequency receiver consists of three frequency bands designated 1, 2, and 3, each covering a 3 octave frequency range. Band 1 is divided into 16 logarithmically spaced frequency channels ($\Delta f/f \simeq 13\%$) and bands 2 and 3 each have 32 frequency channels ($\Delta f/f \simeq 7\%$). During the Jupiter Langmuir wave observations discussed in this paper, the MFR is attached to the E_w monopole, and for the Saturn observations discussed in this paper, the MFR is attached to the E_x dipole.

3 Cassini Observations

3.1 Venus

Two gravity assist flybys of Venus were employed by Cassini during its seven year flight to Saturn. During the first (DOY 116, 1998), the RPWS instrument was operated in a simple high-frequency mode to search for lightning [Gurnett et al., 2001], resulting in no observations of Langmuir waves. During the second flyby on DOY 175, 1999, RPWS was operated in a more typical mode, allowing good lower-frequency plasma wave data (including Langmuir waves) to be obtained. Panel (a) of Figure 1 shows the trajectory of the second Venus flyby. During this flyby, Cassini approached Venus along the Venusian flank and exited the Venusian system near the nose of the bow shock. Panel (a) of Figure 2 shows a time-frequency spectrogram obtained by RPWS during this flyby. Langmuir waves at about 30 kHz were detected as Cassini traveled along the Venusian flank (from about 19:20 to 20:20 SCET). Cassini crossed the bow shock outbound at about 20:40 SCET, and intense Langmuir waves were detected at about 20 kHz as soon as Cassini entered the solar wind. This change in frequency between the inbound and outbound part of the flyby suggests that the solar wind density decreased from about 11cm^{-3} to about 5cm^{-3} while Cassini was close to Venus. The intense band of Langmuir waves observed as Cassini receded from Venus lasted for about 10 minutes, and the sudden drop in the intensity at about 20:50 SCET is probably due to Cassini exiting the electron foreshock region. The Langmuir waves briefly reappear at about 20:52, probably due to a rotation of the solar wind magnetic field causing Cassini to briefly become reconnected to the bow shock (reenter the electron foreshock and encounter the streaming electron beam). Although harmonic structure associated with Langmuir waves has been detected upstream of the Earth [Hoang et al., 1981; Reiner et al., 1996], the emissions detected at harmonics of 20 kHz during this period are believed to be instrumental, caused by

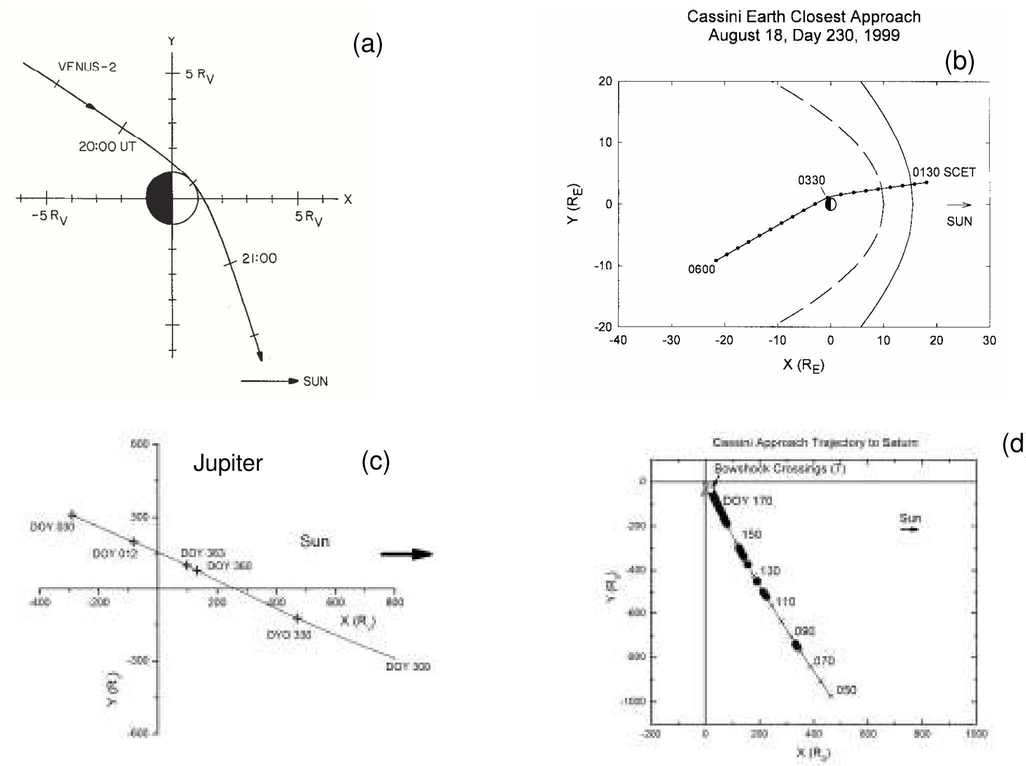

Figure 1: The trajectory of Cassini in the X-Y plane at the second Venus flyby (Panel (a)), Earth (Panel (b)), Jupiter (Panel (c)), and as Cassini approached Saturn (Panel (d)). The sun is to the right in all the panels.

the large amplitudes of the Langmuir waves. The lack of harmonic emissions during the period from 20:50 to 20:52 supports an instrumental effect, since the harmonic emission should be electromagnetic and can propagate outside the foreshock region. Panel (a) of Figure 3 shows the amplitudes ($\mathrm{mV_{peak}m^{-1}}$) measured at 20 kHz during this period immediately after Cassini exited the bow shock (20:39 to 21:16 SCET). The amplitude of the Langmuir waves are on the order of $0.1\mathrm{mV_{peak}m^{-1}}$ immediately after Cassini exits the bow shock, and jumps to a few $\mathrm{mV_{peak}m^{-1}}$ near the foreshock boundary. This variation of the peak electric field is similar to the distribution detected by Galileo [Hospodarsky et al., 1994] where the peak fields were detected near the foreshock boundary.

Panel (a) of Figure 4 shows a histogram of the measured Langmuir wave electric field amplitudes from the period in the box of Panel (a) of Figure 3. The box was drawn to remove measurements near the background noise level of the instrument. However, this selection causes some of the weaker Langmuir waves to be excluded from this histogram. The largest Langmuir wave electric field detected by Cassini during this period was approximately $4.6\mathrm{mV_{peak}m^{-1}}$. This is similar to the peak amplitude of $10\mathrm{mV_{peak}m^{-1}}$ detected by Pioneer Venus [Crawford et al., 1990] and the peak amplitude of $1\mathrm{mV_{peak}m^{-1}}$ detected by Galileo [Hospodarsky et al., 1994].

The dimensionless energy density W, defined as the ratio of the Langmuir wave electric

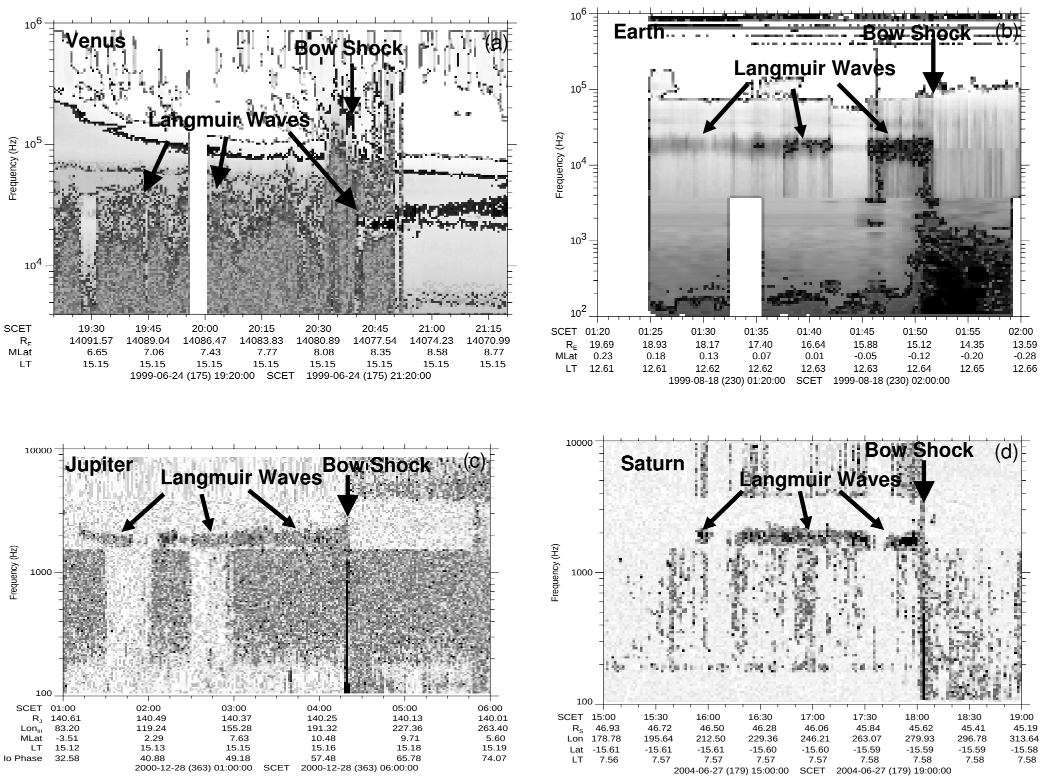

Figure 2: Time-frequency spectrograms of the Langmuir waves detected by Cassini upstream of the bow shock of each planet.

field energy density to the plasma energy density, is used in many studies to characterize the strength of the nonlinear interaction of the Langmuir waves and the plasma. Writing W in terms of the local peak electric fields E_{peak} gives

$$W = \frac{\epsilon_0 E_{peak}^2}{4 n_e k_B T_e} \tag{1}$$

where T_e is electron temperature of the solar wind. Unfortunately CAPS was not operating during the Venus flybys, so no electron temperatures were determined during this flyby. To give a rough estimate of W for the Langmuir waves detected during this flyby, the electron plasma temperature of 3.1×10^5K measured by the Galileo spacecraft during its Venus flyby was used [Frank et al., 1991]. Using this value and a density of 5cm^{-3} obtained from the frequency of the Langmuir waves, the resulting values of W are shown at the top of Panel (a) of Figure 4. This estimation of W for the peak electric field is about a factor of 100 larger than the value obtained by Galileo during its flyby [Hospodarsky et al., 1994]. The large difference in W between the Galileo and Cassini flybys is probably due to the use of the Galileo measurement of T_e.

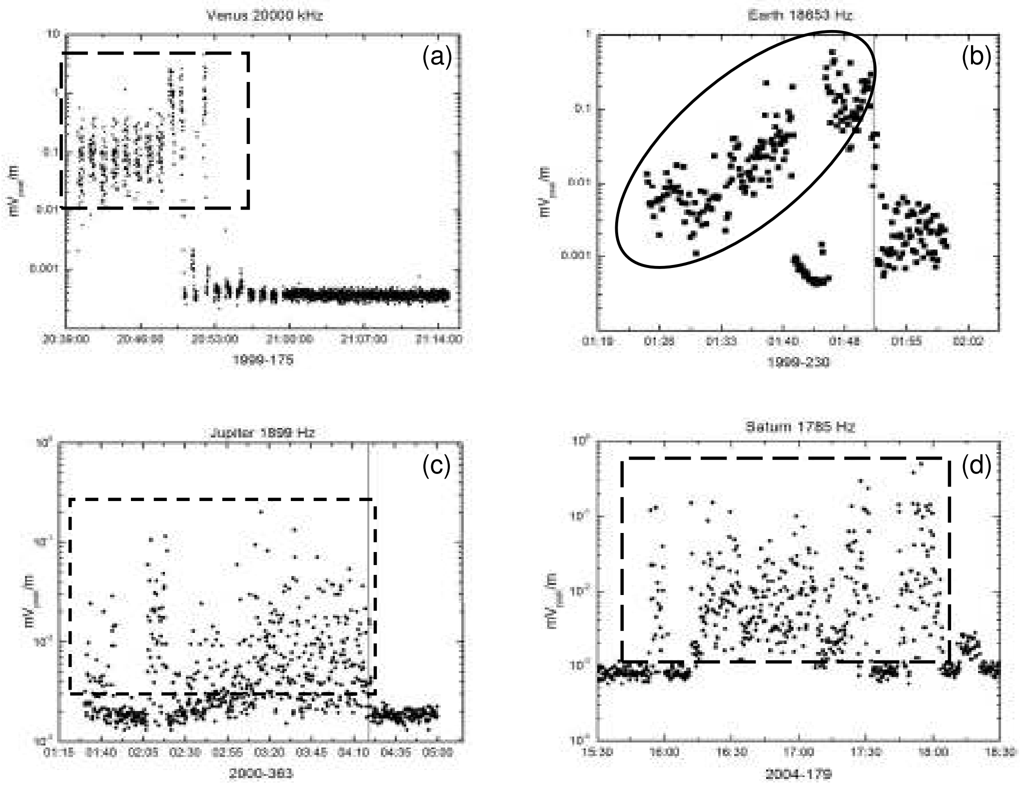

Figure 3: The electric field amplitudes of the Langmuir waves detected by Cassini upstream of the bow shock of each planet. The square and ovals shows the region used to create the histograms in Figure 4.

3.2 Earth

Cassini preformed a gravity assist flyby of the Earth on DOY 230, 1999. Panel (b) of Figure 1 shows the trajectory of the Cassini spacecraft during this flyby. Unlike the Venus 2 flyby where Cassini approached along the flank of Venus and exited near the nose of the Venusian bow shock, Cassini approached the Earth from the sunward side, crossed the bow shock near the nose, and exited along Earth's tail. For a summary of the RPWS observations obtained during of the Earth flyby, see Kurth et al. [2001]. Panel (b) of Figure 2 shows a time-frequency spectrogram of the period as Cassini approached the Earth. A series of Langmuir waves can be seen below about 20 kHz as Cassini approached the bow shock (at about 01:52 SCET). The nearly constant frequency ($\sim$ 19 kHz) of the Langmuir waves implies that the density of the solar wind ($\sim 4.5\text{cm}^{-3}$) was nearly constant during this period. The calculated density of 4.5cm^{-3} from the Langmuir wave frequency agrees well with the average density of 4.6cm^{-3} measured by the Electron Spectrometer from the CAPS instrument [Rymer et al., 2001]. Panel (b) of Figure 3 shows the amplitude of the Langmuir waves detected at 18.7 kHz during this period. The amplitude of the Langmuir waves tended to increase as Cassini approached the bow shock. The reduction of the signal strength from about 01:42 to 01:46 SCET is probably due to Cassini briefly

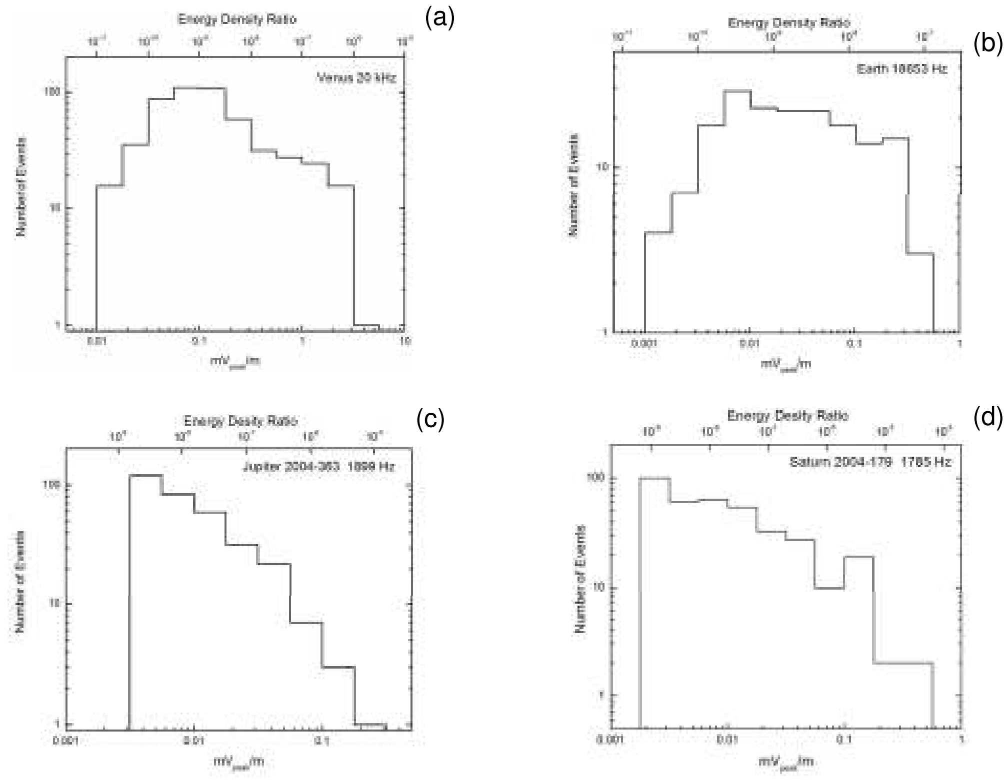

Figure 4: The number measurements as a function of peak electric field strength for each of the planets.

exiting the foreshock region, probably due to a rotation of solar wind magnetic field. The "weak" emissions detected during this period near the plasma frequency are likely thermally excited. For a discussion of thermally excited emissions observed in the solar wind, see Meyer-Vernet and Perche [1989].

Panel (b) of Figure 4 shows a histogram of the Langmuir wave amplitudes shown in the oval from Panel (b) of Figure 3. The largest Langmuir wave electric field detected by Cassini during this period was approximately $0.6 \mathrm{mV_{peak} m^{-1}}$. This value is smaller than the peak fields measured at the Earth by previous spacecraft (typically tens of $\mathrm{mV_{peak} m^{-1}}$) [Cairns et al., 1997, Bale et al., 1997, Sigsbee et al., 2004a, 2004b]. To calculate the energy density ratio of the Langmuir waves during this period, the calculated density of $4.5 \mathrm{cm^{-3}}$ and the electron temperature of $1.2 \times 10^5 \mathrm{K}$ obtained by the CAPS instrument [Rymer et al., 2001] were used, and are shown at the top of Panel (b) of Figure 4.

3.3 Jupiter

Cassini had a gravity assist flyby of Jupiter with closest approach occurring on December 30, 2000. Panel (c) of Figure 1 shows the trajectory of Cassini during the flyby. Cassini approached Jupiter from the morning side, near the nose of the bow shock, and exited down the dusk flank. The first bow shock crossing detected by Cassini occurred on DOY 363, at about 04:20 SCET, with numerous other crossings occurring during the next few months as Cassini traveled along the Jovian dusk flank. For a review of the RPWS results during the Jupiter flyby, with an emphasis on the results in the Jovian dusk flank region, see Kurth et al. [2002]. Panel (c) of Figure 2 shows the time-frequency spectrogram of the period of the first bow shock crossing. The Langmuir waves are the narrowband emission centered at about 1.9 kHz, which gives an solar wind electron density of about 0.045cm^{-3}. This electron density value is on the low end for typical solar wind conditions at Jupiter, suggesting that Cassini was in a region of lower solar wind pressure. Later observations of Langmuir waves during this flyby were often above 10 kHz, implying electron densities of over 1cm^{-3} [see Kurth et al., 2002] for more detailed discussion of the solar wind dynamics and the position of the Jovian bow shock and magnetopause during this flyby].

The amplitude of the Langmuir waves at 1.9 kHz are plotted in Panel (c) of Figure 3. As can be seen, the peak amplitude of the Langmuir waves was about 0.2mV$_{\mathrm{peak}}$m^{-1}. Panel (c) of Figure 4 shows the distribution of the amplitudes shown in the box of Panel (c) of Figure 3. The energy density ratio is plotted on the top of Panel (c) using an electron temperature of 2.3×10^5K provided by the CAPS instrument [Rymer, personal communication, 2005] and the electron density 0.045cm^{-3}.

3.4 Saturn

Cassini approached Saturn in early 2004, with Saturn Orbit Insertion (SOI) occurring on July 1, 2004. Panel (d) of Figure 1 shows the trajectory of Cassini as it approached Saturn. See Gurnett et al. [2005] for a summary of the RPWS results during the approach to Saturn. Langmuir waves associated with the Saturnian bow shock were first detected on DOY 082, 2004, and at a distance of 825 R_s from Saturn. Detection of Langmuir waves continued sporadically as Cassini approached Saturn, becoming almost continuous as Cassini approached the bow shock. The filled-in circles on Panel (d) of Figure 1 show the position of Cassini for each day that Langmuir waves were detected. The detection of Langmuir waves at such a large distance from Saturn is due to the approach trajectory of Cassini being along the dawn side of Saturn, providing a favorable geometry for the solar wind magnetic field to be connected to the Saturnian bow shock, allowing electrons to stream along the magnetic field from the bow shock to Cassini and produce the Langmuir waves. An examination of the magnetic field data shows that for the periods that Langmuir waves are detected by RPWS during approach, the local magnetic field is oriented such that it maps to regions near Saturn. Furthermore, during many of the Langmuir waves events, the CAPS instrument detects 10 to 100 eV electron beams coming from the direction of Saturn.

Cassini crossed the Saturnian bow shock seven times during the approach to Saturn, with the first crossing occurring at about 09:45 SCET on DOY 179. The Langmuir waves detected upstream of each of these bow shocks ranged from about 1.5 kHz to about 3 kHz (solar wind densities from about 0.03 to $0.1cm^{-3}$), implying that the solar wind was dynamic during this period, and also helps explain the multiple bow shock crossings detected by Cassini. Hansen et al. [2005] uses a 3D global magnetohydrodynamic simulation to examine the solar wind/Saturnian magnetosphere interaction during the Cassini approach period. They found good agreement with the first bow shock crossing, but the lack of a time-series of the solar wind velocity (CAPS did not have good pointing during this period to observe the solar wind velocity) resulted in their model missing the other bow shock crossings.

For the analysis of the amplitude of the Langmuir waves, we have selected the period upstream of the third bow shock crossing at about 18:04 SCET, DOY 179, since the Langmuir waves do not vary much in frequency during this period and they tend to be more intense than other periods, possibly due to Cassini being near the foreshock boundary. Panel (d) of Figure 2 shows a time-frequency spectrogram of this period of interest. The Langmuir waves are the narrowband emission at about 1.8 kHz, and the bow shock crossing is the broadband emission from about 100 Hz to 3 kHz at about 18:04 SCET. Panel (d) of Figure 3 shows the $\mathrm{mV_{peak}m^{-1}}$ amplitude of the waves in the 1.785 kHz channel of the RPWS instrument. The amplitude of the Langmuir waves range from about 10^{-3} to $0.5\mathrm{mV_{peak}m^{-1}}$.

Panel (d) of Figure 4 shows the distribution of the amplitudes shown in the box of Panel (d) of Figure 3, with the corresponding energy density ratio shown at the top of the panel. An electron temperature of $2.0 \times 10^5 K$ determined by the CAPS instrument [Achilleous et al. 2005] was used for the solar wind electron temperature, and a electron density of $0.04 cm^{-3}$ was determined from the frequency of the Langmuir waves.

4 Discussion

Langmuir waves have been detected by the RPWS instrument on Cassini upstream of the bow shock of each planet Cassini has visited. The characteristics of the Langmuir waves are similar at each planet, with the main difference being the expected difference in the frequency of the waves due to the decrease in the solar wind density with distance from the sun. The Langmuir waves have similar spectral characteristics at each planet. Usually, near the bow shock crossings, the Langmuir waves are found to be intense, narrowband emissions near the electron plasma frequency. Although not discussed in detail in this study, the Langmuir waves often show spectra that are up- and/or down-shifted in frequency from the plasma frequency, very similar to previous observations by other spacecraft [Etcheto and Faucheux, 1984; Fuselier et al., 1985; Lacombe et al., 1985; Hospodarsky et al., 1994; Lobzin et al., 2005]. Furthermore, the high rate RPWS Wideband (WBR) observations of Langmuir waves obtained at Jupiter and Saturn show very similar fine structure to Langmuir waves observed at Venus by Galileo [Hospodarsky et al., 1994], at the Earth by Galileo [Hospodarsky, 1994] and the Wind spacecraft [Bale et al., 1997], and at Jupiter by the Voyager spacecraft [Gurnet et al., 1981].

The peak electric field amplitudes of the Langmuir waves measured by Cassini are very similar for each of the four planets, ranging from 0.2 to $4.6\mathrm{mV_{peak}m^{-1}}$, and are similar to values obtained by previous spacecraft [Macek et al., 1991]. It should be noted that these peak values are lower limits. The most intense Langmuir waves can occur in packets with structure smaller than the integration time of the HFR and MFR receivers. For example, intense Langmuir waves with structure on the order of 10's of ms has been observed in the Earth's foreshock [Hospodarsky 1994; Bale et al., 1997]. The magnitude of this possible

under estimation of the peak amplitude and the field strength of the small scale packets will be discussed in a future work using the RPWS highrate WBR observations.
Recent work by Boshuizen et al. [2004] using Voyager results has examined the distribution of electric field amplitudes of the Langmuir waves detected at Saturn, Uranus, and Neptune. Their analysis suggests that the distributions support the stochastic growth theory model of Langmuir wave propagation [Robinson, 1995]. However, examinations of the electric field amplitudes at the Earth using WIND data [Bale et al., 1997] found a distribution that did not appear to be consistent with stochastic growth theory. Further analysis of the distribution of the electric field amplitudes of the Langmuir waves presented in this study, and for the other events Cassini encountered at each of the four planets is ongoing.
The peak energy density ratios obtained during the Cassini flybys range from about 1×10^{-7} at Earth to 5×10^{-5} at Saturn. Table 1 summarizes the peak electric field and energy density results for the four periods discussed in this paper and includes the Galileo Venus results. Except for the Cassini Venus flyby (for which a Galileo measurement of the electron temperature was used), the energy density ratio is found to increase with distance from the sun. If the Galileo Venus results replace the Cassini results, then the trend is true for all four planets.

Table 1: Peak electric field and energy density ratio for all four planets

Planet	Peak Electric Field ($mV_{peak}m^{-1}$)	Energy Density Ratio W
Venus (Cassini)	4.6	2×10^{-6}(estimate)
Venus (Galileo)	1.0	2×10^{-8}
Earth	0.6	1×10^{-7}
Jupiter	0.2	6×10^{-6}
Saturn	0.5	5×10^{-5}

Acknowledgments

The research at The University of Iowa is supported by the National Aeronautics and Space Administration through contract 961152 with the Jet Propulsion Laboratory. We acknowledge the support from the Iowa Cassini-RPWS team, especially Terry Averkamp. Cassini-RPWS activities at LESIA are supported by the French CNES (Centre National d'Études Spatiales).

References

Achilleos, N., C. Bertucci, C. T. Russell, G. B. Hospodarsky, A. M. Rymer, C. C. Arridge, M. E. Burton, M. K. Dougherty, S. Hendricks, E. J. Smith, and B. T. Tsurutani, Orientation, location and velocity of Saturn's bow shock: initial results from the Cassini spacecraft, *J. Geophys. Res.*, **111**, A03201, doi:10.1029/2005JA011297, 2006.

Bale, S. D., D. E. Larson, R. P. Lin, P. J. Kellogg, K. Goetz, and S. J. Monson, On the amplitude of intense electron plasma waves in the terrestrial electron foreshock, *J. Geophys. Res.*, **102**, 11281, 1997.

Bale, S. D., D. E. Larson, R. P. Lin, P. J. Kellogg, K. Goetz, and S. J. Monson, On the beam speed and wavenumber of intense electron plasma waves near the foreshock edge, *J. Geophys. Res.*, **105**, 27353, 2000.

Bonnell, J., P. Kintner, J. -E. Wahlund, and J. A. Holtet, Modulated Langmuir waves: Observations from Freja and SCIFER, *J. Geophys. Res.*, **102**, 17233, 1997.

Boshuizen, C. R., I. H. Cairns, and P. A. Robinson, Electric field distributions for Langmuir waves in planetary foreshocks, *J. Geophys. Res.*, **109**, A08101, doi:10.1029/2004JA010408, 2004.

Cairns, I. H., P. A. Robinson, R. R. Anderson, and R. J. Strangeway, Foreshock Langmuir waves for unusually constant solar wind conditions, *J. Geophys. Res.*, **102**, 24249, 1997.

Crawford, G. K., R. J. Strangeway, and C. T. Russell, Electron plasma oscillations in the Venus foreshock, *Geophys. Res. Lett.*, **17**, 1805, 1990.

Etcheto, J., and M. Faucheux, Detailed study of electron plasma waves upstream of the Earth's bow shock, *J. Geophys. Res.*, **89**, 6631, 1984.

Filbert, P. C., and P. J. Kellogg, Electrostatic noise at the plasma frequency beyond the Earth's bow shock, *J. Geophys. Res.*, **84**, 1369, 1979.

Frank, L. A., W. R. Paterson, K. L. Ackerson, F. V. Coroniti, V. M. Vasyliunas, Plasma observations at Venus with Galileo, *Science*, **252**, 1528, 1991.

Fuselier, S. A., D. A. Gurnett, and R. J. Fitzenreiter, The downshift of electron plasma oscillations in the electron foreshock region, *J. Geophys. Res.*, **90**, 3935, 1985.

Gurnett, D. A., J. E. Maggs, D. L. Gallagher, W. S. Kurth, and F. L. Scarf, Parametric interaction and spatial collapse of beam-driven Langmuir waves in the solar wind, *J. Geophys. Res.*, **86**, 8833, 1981.

Gurnett, D. A., P. Zarka, R. Manning, W. S. Kurth, G. B. Hospodarsky, T. F. Averkamp, M. L. Kaiser, W. M. Farrell, Non-Detection at Venus of high-frequency radio signals characteristic of Terrestrial lighting, *Nature*, **409**, 313, 2001.

Gurnett, D. A., W. S. Kurth, D. L. Kirchner, G. B. Hospodarsky, T. F. Averkamp, P. Zarka, A. Lecacheux, R. Manning, A. Roux, P. Canu, N. Cornilleau-Wehrlin, P. Galopeau, A. Meyer, R. Bostrom, G. Gustafsson, J.-E. Wahlund, L. Aahlen, H. O. Rucker, H. P. Ladreiter, W. Macher, L. J. C. Woolliscroft, H. Alleyne, M. L. Kaiser, M. D. Desch, W. M. Farrell, C. C. Harvey, P. Louarn, P. J. Kellogg, K. Goetz, and A. Pedersen, The Cassini radio and plasma wave science investigation, *Space Sci. Rev.*, **114**, 395, 2004.

Gurnett, D. A., W. S. Kurth, G. B. Hospodarsky, A. M. Persoon, T. F. Averkamp, B. Cecconi, A. Lecacheux, P. Zarka, P. Canu, N. Cornilleau-Wehrlin, P. Galopeau,

A. Roux, C. Harvey, P. Louarn, R. Bostrom, G. Gustafsson, J.-E. Wahlund, M. D. Desch, W. M. Farrell, M. L. Kaiser, K. Goetz, P. J. Kellogg, G. Fischer, H.-P. Ladreiter, H. Rucker, H. Alleyne, and A. Pedersen, Radio and plasma wave observations at Saturn from Cassini's approach and first orbit, *Science*, **307**, 1255, 2005.

Hoang, S., J. Fainberg, J. -L. Steinberg, R. G. Stone, and R. H. Zwickl, The $2f_p$ circumterrestrial radio radiation as seen from ISEE 3, *J. Geophys. Res.*, **86**, 4531, 1981.

Hospodarsky, G. B., D. A. Gurnett, W. S. Kurth, M. G. Kivelson, R. J. Strangeway, and S. J. Bolton, The fine structure of Langmuir waves observed upstream of the bow shock at Venus, *J. Geophys. Res.*, **99**, 13363, 1994.

Hospodarsky, G. B., An analysis of the fine structure of Langmuir wave emissions, Thesis (Ph.D.), University of Iowa, 1996.

Kinter, P. M., J. Bonnell, S. Powell, and J. -E. Wahlund, First results from the Freja HF Snapshot Receiver, *Geophys. Res. Lett.*, **22**, 287, 1995.

Kurth, W. S., G. B. Hospodarsky, D. A. Gurnett, M. L. Kaiser, J.-E. Wahlund, A. Roux, P. Canu, P. Zarka, and Y. Tokarev, An Overview of Observations by the Cassini Radio and Plasma Wave Investigation at Earth, *J. Geophys. Res.*, **106**, 30,239, 2001.

Kurth, W. S., D. A. Gurnett, G. B. Hospodarsky, W. M. Farrell, A. Roux, M. K. Dougherty, S. P. Joy, M. G. Kivelson, R. J. Walker, F. J. Crary, and C. J. Alexander, The dusk flank of Jupiter's magnetosphere, *Nature*, **451**, 991, 2002.

Lacombe, C. A., A. Mangency, C. C. Harvey, and J. D. Scudder, Electron plasma waves upstream of Earth's bow shock, *J. Geophys. Res.*, **90**, 73, 1985.

Lobzin, V. V., V. V. Krasnoselskikh, S. J. Schwarts, I. Cairns, B. Lefebvre, P. Decreau, and A. Fazakerley, Generation of downshifted oscillations in the electron foreshock: A loss-cone instability, *Geophys. Res. Lett.*, **32**, L18101, doi:10.1029/2005GL023563, 2005.

Macek, W. M., I. H. Cairns, W. S. Kurth, and D. A. Gurnett, Plasma wave generation near the inner heliospheric shock, *Geophys. Res. Lett.*, **18**, 357, 1991.

Meyer-Vernet, N., and C. Perche, Tool kit for antennae and thermal noise near the plasma frequency, *J. Geophys. Res.*, **94**, 2405, 1989. Robinson, P. A., Stochastic wave growth, *Phys. Plasmas*, **2**, 1466, 1995.

Reiner, M. J., M. L. Kaiser, J. Fainberg, M. D. Desch, and R. G. Stone, $2f_p$ radio emission from the vicinity of the Earth's foreshock: WIND observations, *Geophys. Res. Lett.*, **23**, 1247, 1996.

Rymer, A. M., A. J. Coates, K. Svenes, G. A. Abel, D. R. Linder, B. Narheim, M. Thomsen, and D. T. Young, Cassini Plasma Spectrometer Electron measurements during the Earth swing-by on August 18, 1999, *J. Geophys. Res.*, **106**, 30,177, 2001.

Sigsbee, K., C. A. Kletzing, D. A. Gurnett, J. S. Pickett, A. Balogh, and E. Lucek, The dependence of Langmuir wave amplitudes on position in the Earth's foreshock, *Geophys. Res. Lett.*, **31**, L07805, 2004a.

Sigsbee, K., C. A. Kletzing, D. A. Gurnett, J. S. Pickett, A. Balogh, and E. Lucek, Statistical behavior of foreshock Langmuir waves observed by the Cluster wideband data plasma wave receiver,*Annales Geophysicae*, **22**, 2337, 2004b.

Soucek, J., V. Krasnoselskikh, T. Dudok de Wit, J. Pickett, and C. Kletzing, Nonlinear decay of foreshock Langmuir waves in the presence of plasma inhomogeneities: Theory and Cluster observations, *J. Geophys. Res.*, **110**, A08102, doi:10.1029/2994JA010977, 2005.